
Blob transport at high collisionality and the SOL density limit

D. A. D'Ippolito, J. R. Myra, and D. A. Russell
Lodestar Research Corporation

*Presented at the 33rd EPS Conference on Plasma Physics,
Rome, Italy, June 19 - 23, 2006*

Summary and Conclusions

- n **Coherent structures (“blobs”)** created by edge turbulence \Rightarrow convective transport of particles and heat across the SOL

- n Experiments, simulations and theory show that the **transport rate increases with collisionality**.
 - q increased collisionality Λ (and resistivity $\eta_{||}$) \Rightarrow strong ballooning (disconnection from sheaths) \Rightarrow faster ExB drift
 - q **new 2-region 2D code** encapsulates the essential physics \Rightarrow reduced connection to sheaths, larger turbulent flux at high Λ

- n A **correspondence rule** ($\gamma \rightarrow v_x/a_b$) has been exploited to understand **new regimes of blob transport**
 - q includes collisionality and geometry dependence
 - q valid in near SOL and edge region (blob birth zone)
 - q **blob transport \sim mixing length transport** in edge plasma at high Λ

- n **2-region thermal equilibrium model** gives good agreement with C-Mod experiments
 - q **convective density limit (CDL)** due to thermal instability
 - q CDL corresponds to $q_{\perp} > q_{\parallel}$ in edge plasma
 - q occurs at high collisionality

- n The **general picture** from all of this work is that:
 - q the distinction between edge and SOL disappears at high collisionality because of shorter $L_{\parallel} \sim \lambda_{ei}$
 - q edge transport increases dramatically and can be estimated using collisional blob models with “packing fraction” ~ 1

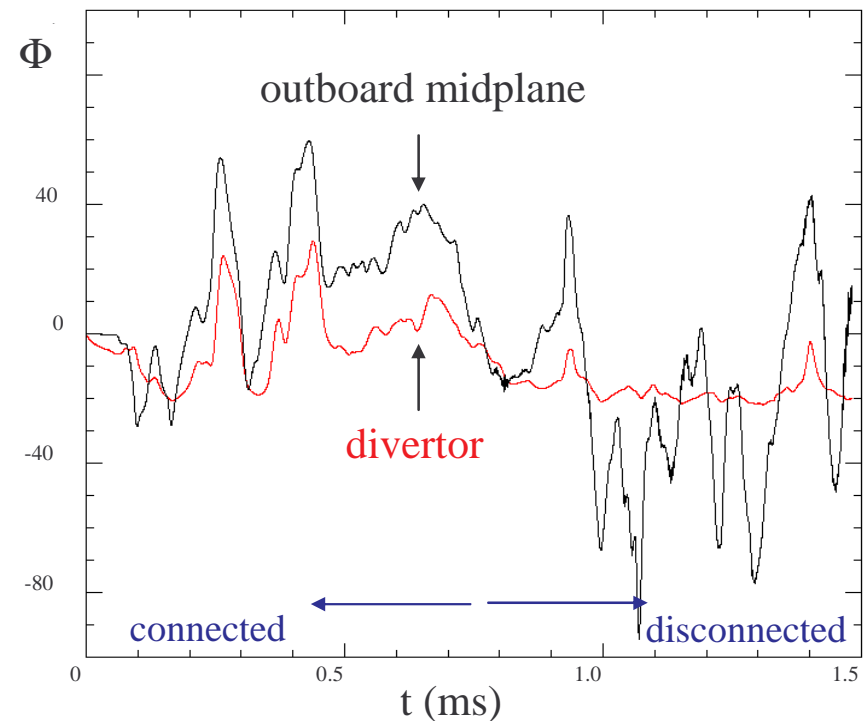
3D BOUT turbulence simulations show faster blobs at higher collisionality

BOUT simulation with $\delta n/n \sim 1$
by X. Xu (2003);

Blob analysis by D. Russell
(2004)

⇒ 3D structure is
important!

- density and collisionality Λ increase with time (gas puffing)
- blobs disconnect from divertor region and move faster as η_{\parallel} and Λ increase



Russell et al, Phys. Rev. Lett 2004

Physical picture: linear growth rate, blob velocity and turbulent transport increase with $\eta_{\parallel} \propto v_e \propto \Lambda$

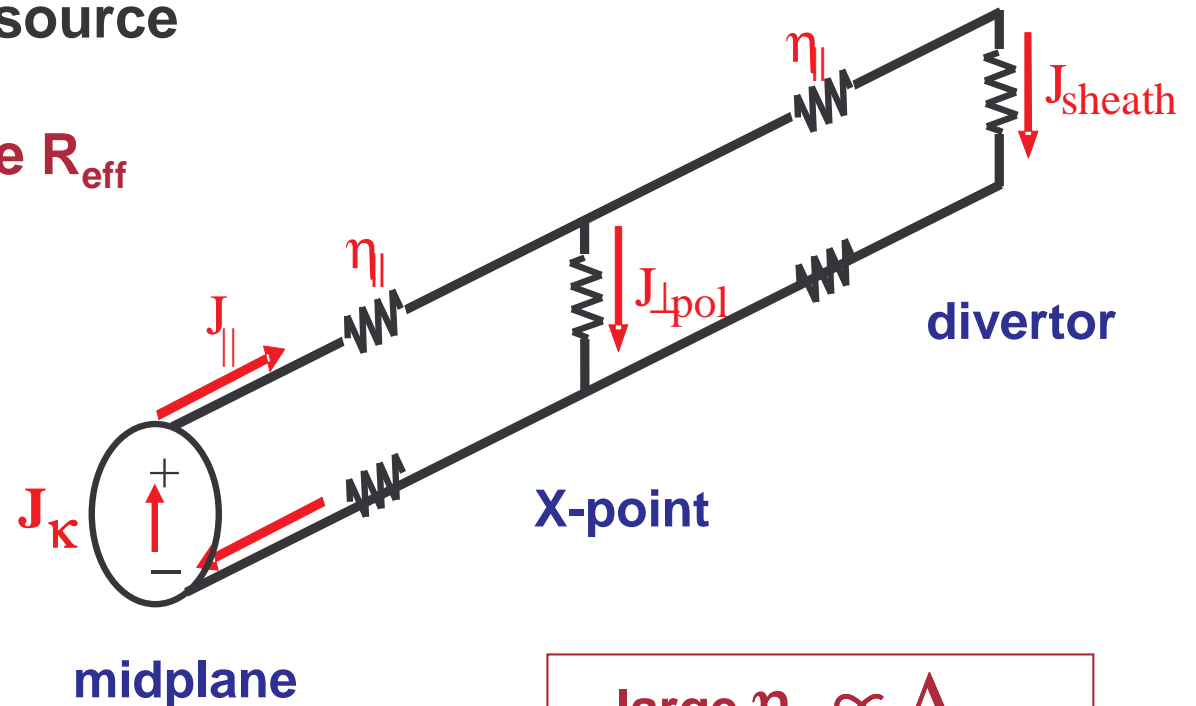
Curvature drift \Rightarrow current source

Effective circuit resistance R_{eff}

\Rightarrow potential $\Phi \sim R_{\text{eff}} J_{\kappa} L_{\parallel}$

\Rightarrow growth rate γ (linear)

\Rightarrow $\mathbf{E} \times \mathbf{B}$ speed v_x (blob)



large $\eta_{\parallel} \propto \Lambda$
 \Rightarrow disconnection

Blob transport and mixing length estimate

In the edge plasma, the blob and mixing length transport estimates agree in order of magnitude provided that the blob “packing fraction” ~ 1 (skewness ~ 1) and we use the “**blob correspondence rule**” (see next page).

Mixing length estimate:

$$\tilde{v}_x \sim i k_{\perp} \tilde{\Phi} , \quad \tilde{n} / n_0 \sim k_{\perp} \tilde{\Phi} / (\omega L_n) ,$$

$$\begin{aligned} \text{Use saturation condition: } \omega &\sim k_{\perp} \tilde{v}_{\perp} \Rightarrow \tilde{\Phi} \sim \omega / k_{\perp}^2 \\ &\Rightarrow \Gamma \sim \text{Re}[\tilde{n} \tilde{v}_x^*] \sim n_0 \gamma / (k_{\perp}^2 L_n) \end{aligned}$$

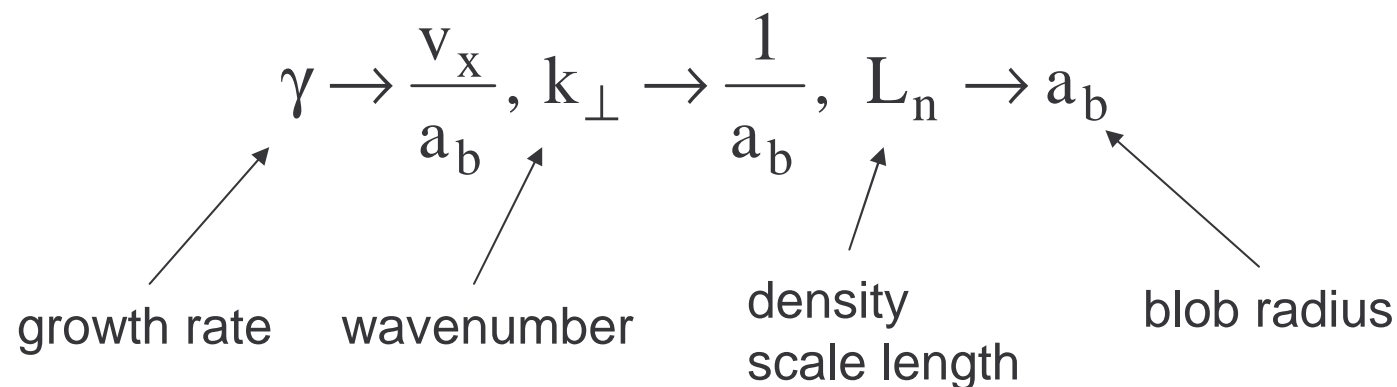
Blob estimate:

$$\Gamma \sim n_b v_x \quad \text{where } n_b \sim n_0 \quad \text{and } v_x \sim \gamma a_b \quad (\text{correspondence rule})$$

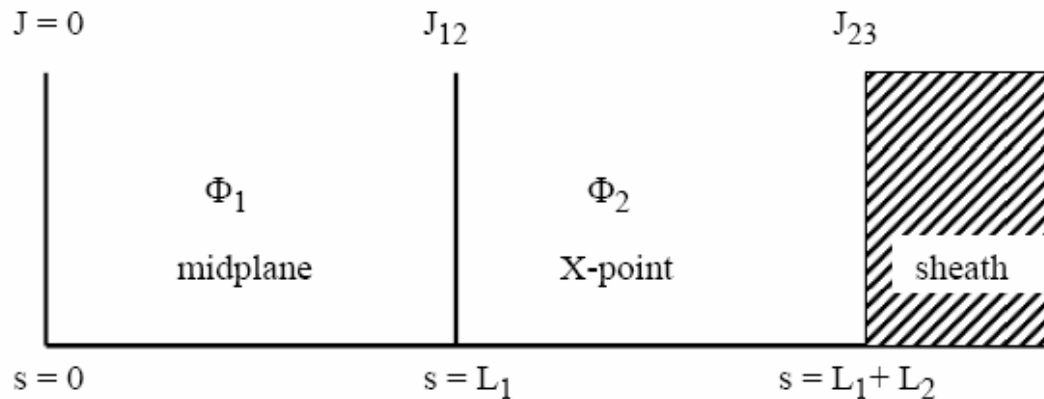
Using the correspondence rule, both estimates agree.

Correspondence rule between linear instability and nonlinear blob physics

- n As noted by *Endler et al. (NF 1995)* for sheath-interchange modes, there is a correspondence between the linear instability and the resulting turbulence.
- n For all instabilities that saturate by wave breaking ($\omega \sim \mathbf{k} \cdot \tilde{\mathbf{v}}$) we postulate the following **correspondence rule** between the instability and the blob velocity:



Two-region 2D model for studying transition to collisional, disconnected regimes



Notes:

- similar eqs. for T_j , but $\mathbf{T} = \text{const.}$ here
- **Bohm units** (dimensionless)

charge

$$n_1 \frac{d}{dt} \nabla_{\perp 1}^2 \Phi_1 = J_{12} / L_1 - \beta \frac{\partial n_1}{\partial y} \quad n_2 \frac{d}{dt} \nabla_{\perp 2}^2 \Phi_2 = (J_{23} - J_{12}) / L_2$$

$$J_{\perp \text{pol}} : J_{\parallel} : \text{curvature} \quad J_{\perp \text{pol}} : J_{\parallel \text{sh}} : J_{\parallel}$$

density

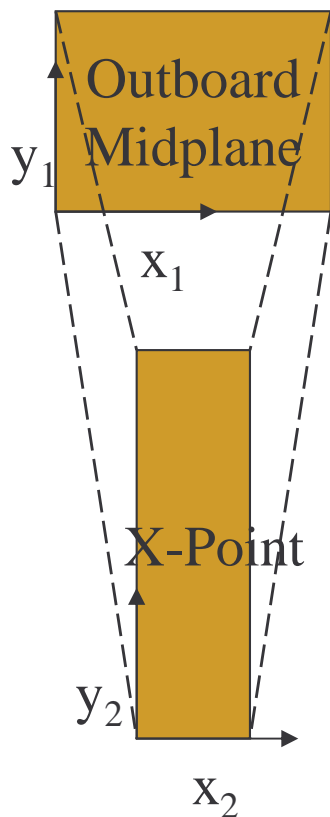
$$\frac{dn_1}{dt} + \Gamma_{12} / L_1 = 0, \quad \Gamma_{12} = n_1 c_{s1}, \quad \frac{dn_2}{dt} = (\Gamma_{12} - \Gamma_{23}) / L_2, \quad \Gamma_{23} = n_2 c_{s2},$$

$$\frac{d}{dt} = \frac{\partial}{\partial t} + \mathbf{v} \cdot \nabla$$

$$J_{12} = \frac{-\sigma_{12}}{L_{12}} (\Phi_2 - \Phi_1), \quad J_{23} = n_2 \alpha \Phi_2$$

Cross-field conductivity is enhanced in region 2 (X-pt) by field line fanning f

- Field lines from midplane region $(x, y)_1$ are mapped to stretched / squeezed coordinates in X-point region $(x, y)_2$ by “fanning factor” $f \ll 1$. At present the model neglects magnetic shear.



$$\frac{\partial}{\partial x_2} = f \frac{\partial}{\partial x_1} \quad , \quad \frac{\partial}{\partial y_2} = \frac{1}{f} \frac{\partial}{\partial y_1} \quad .$$

- charge is conserved between regions 1 and 2
- sheath boundary conditions are applied at the end of region 2

$$J_{\parallel} = nec_s \left(1 - e^{-e(\Phi - \Phi_0)/T_e} \right) \approx 3T_e$$

The model equations are invariant under a scale transformation

$$\begin{aligned} \phi &\rightarrow \lambda\phi, \quad t \rightarrow \lambda^{2\mu-3}t, \quad \mathbf{x} \rightarrow \lambda^{\mu-1}\mathbf{x} \\ \sigma &\rightarrow \lambda^{5-4\mu}\sigma, \quad \text{for arbitrary } \lambda, \mu \\ (\rho_s / R, L_{\parallel} / R) &\rightarrow \lambda^{5-3\mu}(\rho_s / R, L_{\parallel} / R) \end{aligned}$$

invariant scaling method:
Connor & Taylor, Phys.
Fluids 1984

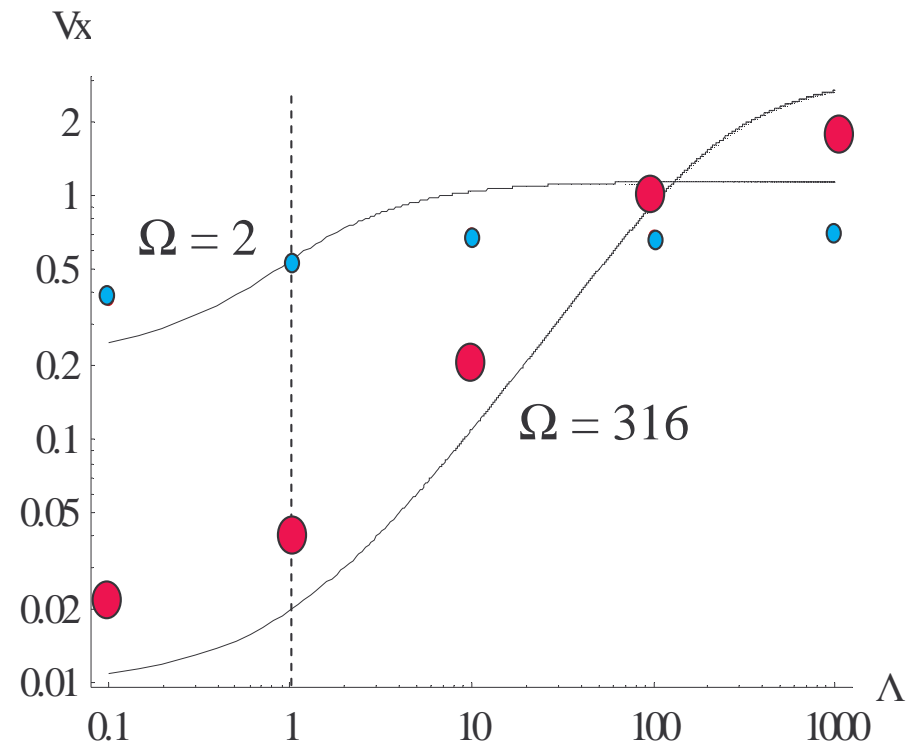
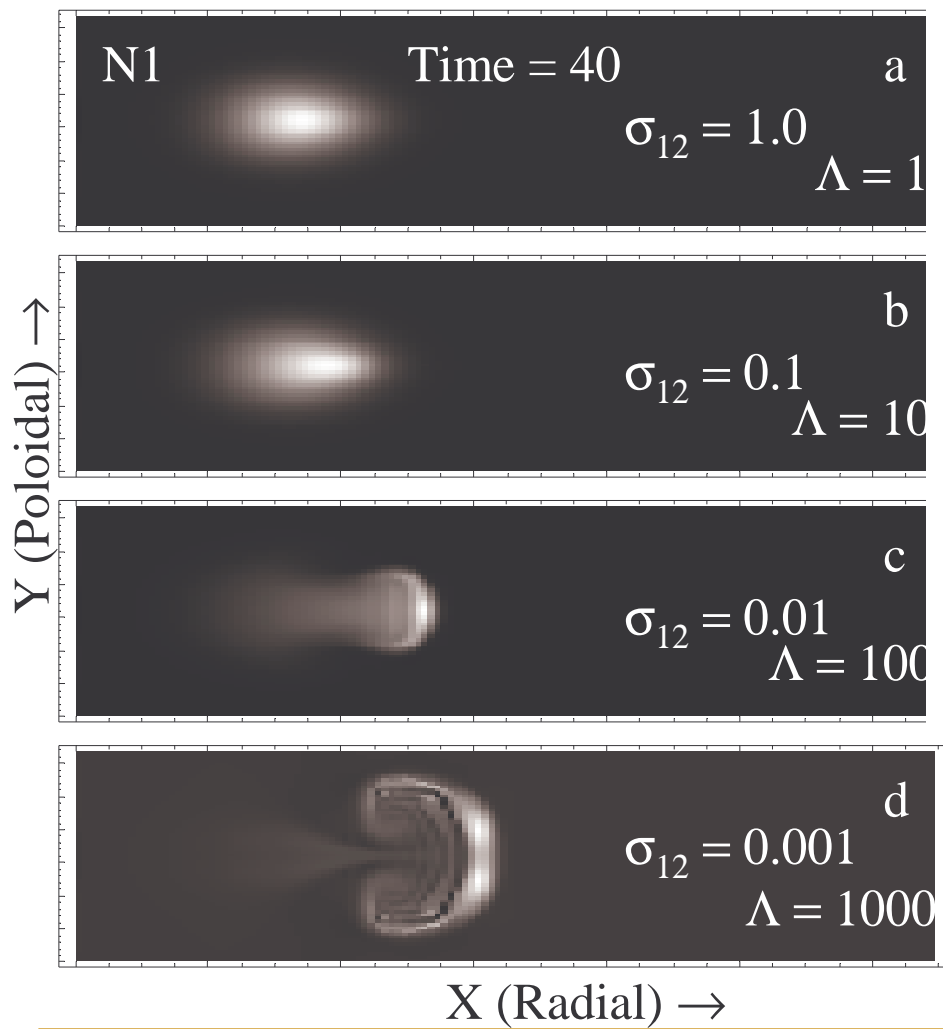
- n the following **invariant combinations** characterize the dimensionless parameter space ($\Lambda =$ collisionality, $\Omega =$ scale size)

$$\Lambda = \frac{\omega_{\eta 1} \omega_{s 1}}{\omega_{a 1}^2} = \frac{v_e L_{\parallel}}{\Omega_e \rho_s}, \quad \Omega = \frac{\omega_{s 1}}{\gamma_{\text{mhd}}} = \left(\frac{L_n R}{L_{\parallel}^2} \right)^{1/2} \frac{1}{k_{\perp 1}^2 \rho_s^2},$$

- n dispersion relation can be written as $\hat{\omega} \equiv \frac{\omega}{\gamma_{\text{mhd}}} = \hat{\omega}[\Lambda, \Omega(k), \varepsilon]$

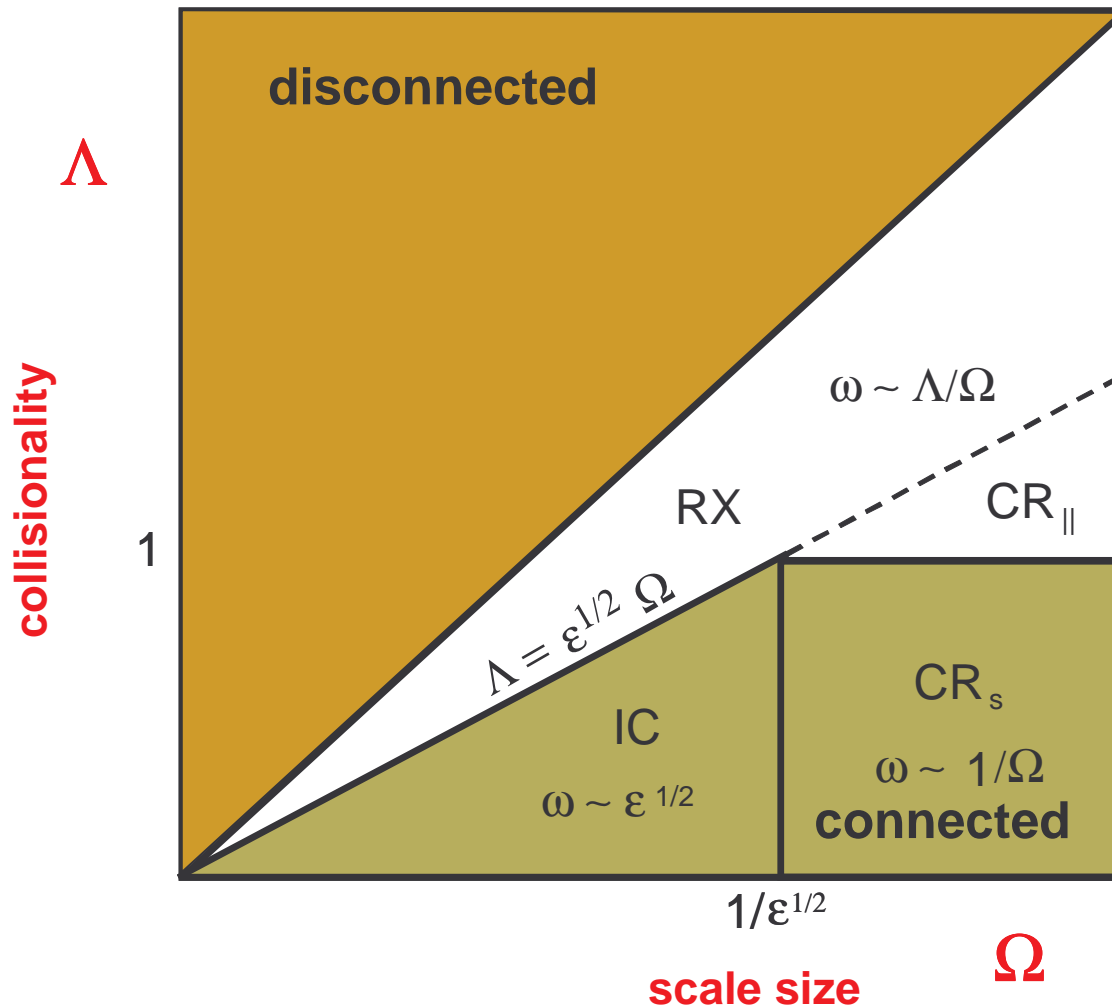
- n **same dispersion relation applies to blobs using the correspondence rule: $\omega \rightarrow v_x/a_b$ and $L_n, 1/k_{\perp} \rightarrow a_b$**

2-region code (with initialized blobs) shows good agreement with blob “dispersion relation” scaling



- n blobs speed up with increasing collisionality Λ (\propto resistivity)
- n for low Λ , small blobs move fastest (nb: $\Omega = (a_b/a_*)^{5/2} \sim$ blob size)

Linear instability / blob regimes



- electrostatic 2-region model

- $\Omega = (a_b/a_*)^{5/2}$

- $a^* = \rho_s^{4/5} L_{||}^{2/5} / R^{1/5}$

- $\epsilon \equiv \epsilon_x^2 = f^2 =$

X-pt fanning factor

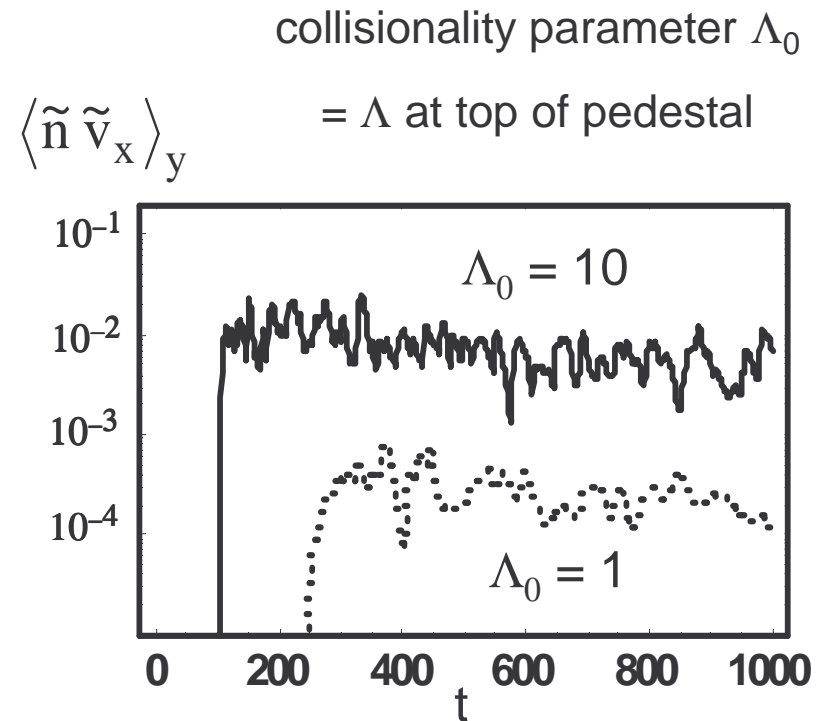
Turbulence simulations: particle transport in two-region code

The two-region fluid turbulence code predicts an **increase in turbulent particle flux with collisionality**, as seen in experiments.

Figure: Time history of the turbulent (blob) particle flux Γ for two values of the collisionality parameter Λ_0 with $f = 1/4$.

Γ is averaged over poloidal direction y for a fixed radial point in the SOL.

Note the earlier onset of the nonlinear turbulent phase and the much larger particle flux for large Λ_0 .



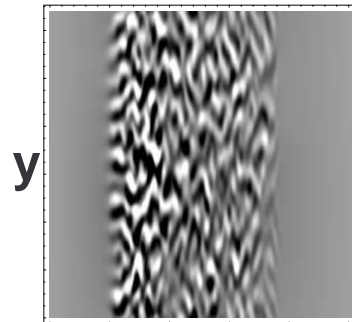
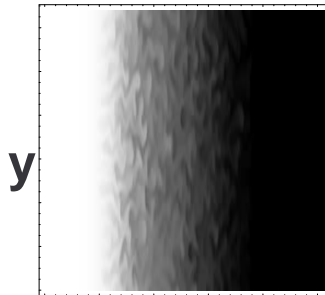
D. Russell (2006)

Turbulence simulations: edge / SOL turbulence & blob structure depend on collisionality

$n_1(x,y)$

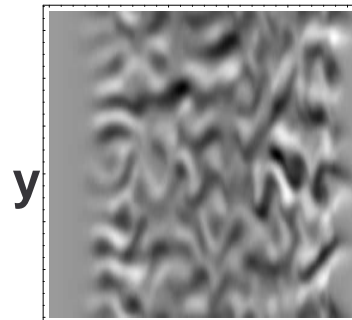
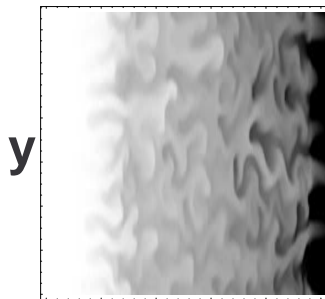
$\phi_1(x,y)$

$\Lambda_0 = 1$



$f = 1/4, \beta = 1, \sigma_{23} = 1, t = 1000$

$\Lambda_0 = 10$

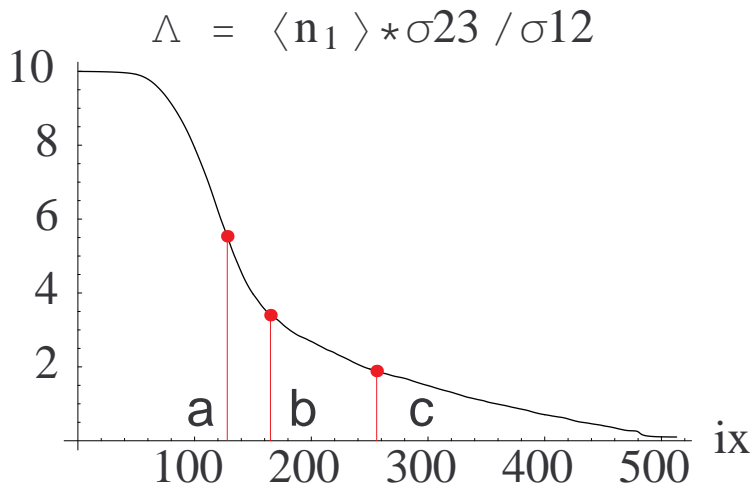


Note: more blobs and faster v_x as Λ_0 increases

D. Russell (2006)

blobs

Disconnection caused by high local collisionality Λ



max $\nabla(\ln n)$ at $x = b$

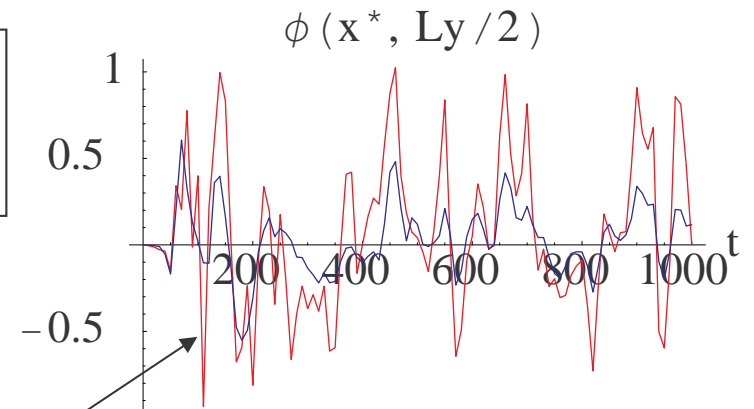
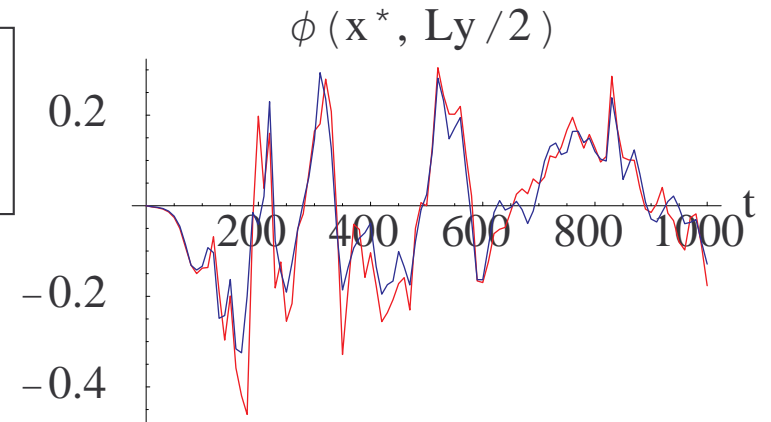
$f = 1/4, \beta = 1, \sigma_{23} = 1$

Red: midplane
Blue: X-point

$\Lambda_0 = 1$
 $\Lambda \approx 0.3$

$\Lambda_0 = 10$
 $\Lambda \approx 3$

$\phi_1(t), \phi_2(t) |_{x,y}$ at $x = b$



partially disconnected: $\phi_1(t) > \phi_2(t)$

D. Russell (2006)

SOL density limit due to blob heat transport

In this work, we include heat transport in an analytic 2-region model for (Φ, T_e) with $n_1, n_2 = \text{const.}$

⇒ **SOL thermal equilibrium limit** ⇒ **density limit**

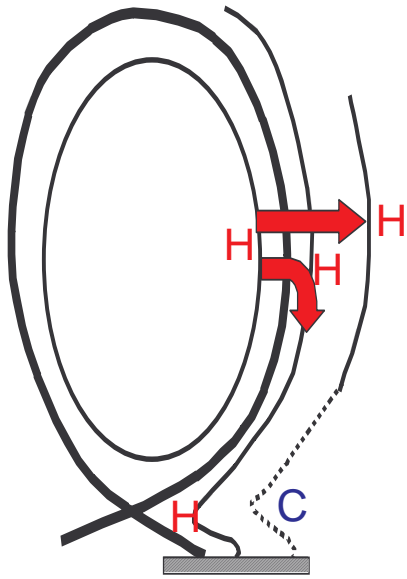
higher density ⇒ higher collisionality
⇒ faster radial heat transport ⇒ lower T
⇒ thermal instability ⇒ thermal collapse of SOL

n C-Mod observes **convective density limit (CDL)** with $q_{\perp} > q_{\parallel}$

n our model ⇒ **CDL when q_{\perp} increases as X-point cools**

(thermal instability analogous to MARFE with radiative cooling → radial convection) (*D'Ippolito and Myra, Phys. Plasmas, June, 2006*)

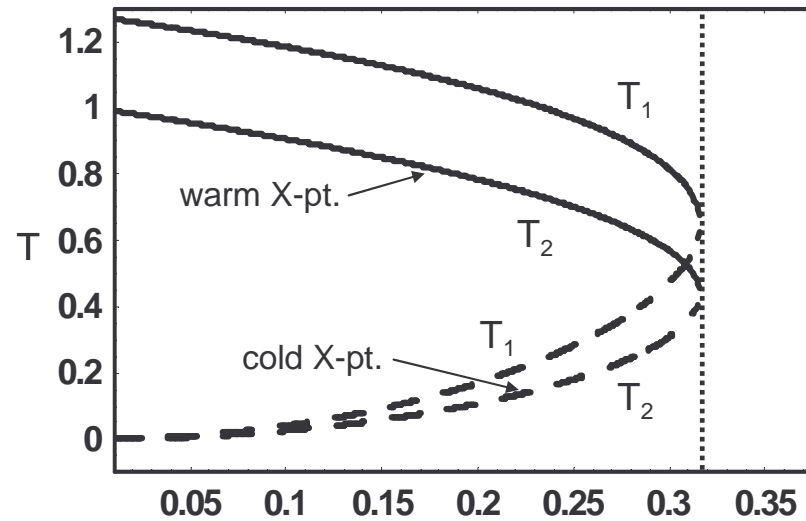
Physical picture is supported by calculation



warm X-pt root (solid) is thermally stable

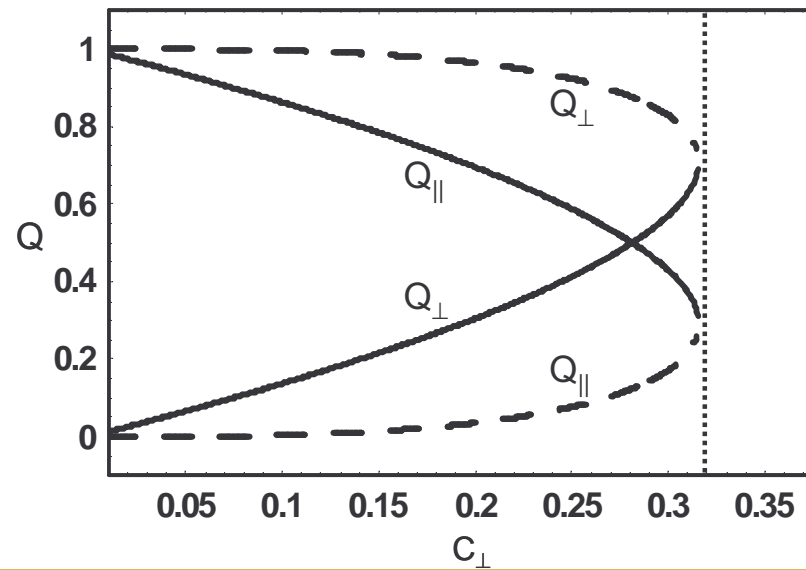
cold X-pt root (dashed) is unstable \Rightarrow thermal instability of SOL

root coalescence = CDL



$T_1 =$ midplane,
 $T_2 =$ X-pt

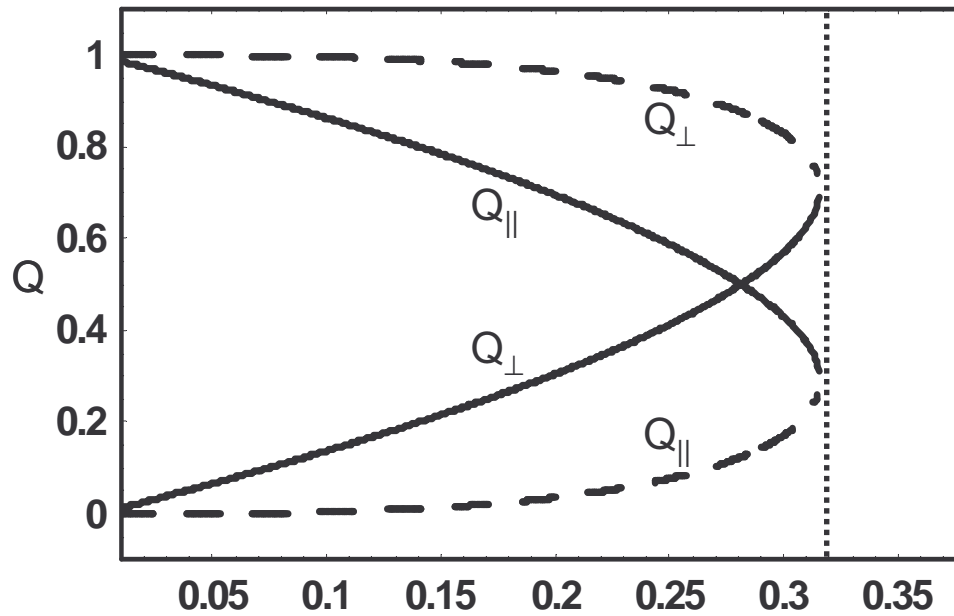
$C_{\perp} \perp$ heat convection \rightarrow



C_{\parallel} fixed

2-region thermal equilibrium model qualitatively agrees with C-Mod density limit experiments

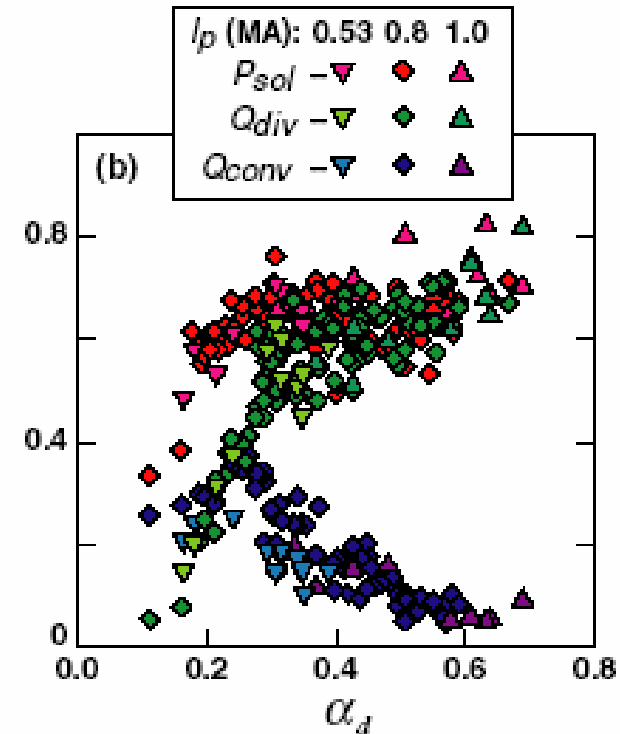
Model



⊥ heat convection → C_{\perp}

$$\alpha_d \propto \left(\frac{1}{\Lambda}\right)^{1/2} \propto \left(\frac{1}{C_{\perp}}\right)^{1/2}$$

C-Mod data



LaBombard et al, NF 2005